

# Influence of mechanical stress on electron field emission of multiwalled carbon nanotube–polymer composites

C. H. P. Poa,<sup>a)</sup> R. C. Smith, and S. R. P. Silva

*Nano-Electronics Centre, Advanced Technology Institute, University of Surrey, Guildford, Surrey GU2 7XH, United Kingdom.*

C. Q. Sun

*School of Electrical and Electronic Engineering, Nanyang Technological University, Singapore 639798*

(Received 24 September 2004; accepted 10 January 2005; published 6 April 2005)

Field emission properties of carbon nanotubes under mechanical stress have been investigated. The emission threshold fields initially decrease from 2.3 to 0.6 V/ $\mu\text{m}$  before rising back to 3.1 V/ $\mu\text{m}$  with increasing mechanical stress applied externally to the film. This behavior from nanotube composites has not been reported and is believed to be associated with modification to the work function of the nanotubes. This work suggests a possible application for these composite films as electromechanical high power switches. © 2005 American Vacuum Society.

[DOI: 10.1116/1.1868692]

## I. INTRODUCTION

Carbon nanotubes (CNTs) are one dimensional materials with outstanding mechanical and electronic properties. Theoretical predictions on single-walled nanotubes (SWNTs) suggest an in-plane elastic modulus equal to a graphene sheet of  $\sim 1060$  GPa.<sup>1</sup> This is comparable to the hardest natural (001) diamond of 1050 GPa. Electron transportation in SWNTs depends on their chirality and diameter, which results in either metallic or semiconducting properties. With ideal electrical contacts, a metallic SWNT can behave like a quantum wire, yielding two units of quantum conductance ( $G=2 G_0=4 e^2/\hbar$ ) and hence ballistic transport.<sup>2</sup> Another potential application with considerable interest is using CNTs as a field emission cathode. Due to its large aspect ratio and tube-like shape, CNTs are excellent electron field emitters which are suitable for cold cathodes in display applications. In fact, low emission threshold fields and high current densities have been obtained from CNTs. More recently, studies have illustrated the combination of using both mechanical and electronic properties of CNTs, such as examining bending and stressing of CNTs for electronic applications.<sup>3–5</sup> Atomic force microscopy tips were used as point-like gates to modulate the conductance of SWNT.<sup>5</sup> By applying strain at a localized point along a SWNT, the conductance decreases by a few orders of magnitude, suggesting the possibility of using this technique for a nanoscale pressure sensor.

Simulations have shown that the band gap of SWNTs vary linearly with stress ( $\sigma$ ), with a ratio of  $|dE_{\text{gap}}/d\sigma|=10.7$  meV/GPa.<sup>6</sup> Using a modified semiempirical, tight-binding approach and introducing a deformation potential, a semiconductor to metal transition was predicted when  $\sigma$  is greater than 10 GPa.

The study of electronic properties with mechanical stress is important in view of the ability to manipulate carbon

nanotubes. Additionally, it is interesting to investigate the field emission properties when mechanical stress is applied. In this article, the electron field emission (FE) properties of multiwalled carbon nanotube (MWNT) composite films were investigated as a function of applied mechanical stress.

## II. EXPERIMENTAL SETUP

The MWNT composite films were prepared by mixing purified MWNTs (8 wt % concentration) with polystyrene (PS). Sample preparation has been described previously in Ref. 7. Briefly, the MWNTs were synthesised using a dc arc discharge technique. Two graphite rods were used as electrodes in a water-cooled vacuum chamber. Helium gas was introduced into the chamber to a process pressure of 100 Torr and an arc was struck with a high current (120 A) power supply. The as-produced MWNTs comprise of a mixture of small carbon particles with amorphous carbon, and no metal particles/catalysts observed in the tubes. The carbon mixture was first purified using microfiltering to remove carbon particles and mild oxidation at 400 °C to remove unwanted amorphous carbon. After purification, MWNTs were mixed with PS in toluene, with the mixture then ultrasonicated for 60 min before transferring to a vacuum chamber for drying. To ensure good dispersion of CNTs and removal of voids in the composite films, the hardened mixtures were subject to “hot pressing.” Finally, the CNT–PS films were cut into dimensions of  $4 \times 25$  mm, and a film thickness of about 250  $\mu\text{m}$ . Figure 1(a) shows an image of the MWNT–PS film surface magnified to 6500 times in a scanning electron microscope. MWNTs can be seen sticking out across the PS surface. The distribution of the MWNTs on the surface appears patchy and selective in Fig. 1(a), but the overall distribution is considered to be even over a sample area of 100 mm<sup>2</sup>. In Fig. 1(b), the sample was intentionally broken into half to form a “hairy fracture.” The cross-sectional view of the composite film shows that MWNTs are well dispersed in the PS matrix and are uniaxially oriented.

<sup>a)</sup>Electronic mail: patrick.poa@surrey.ac.uk

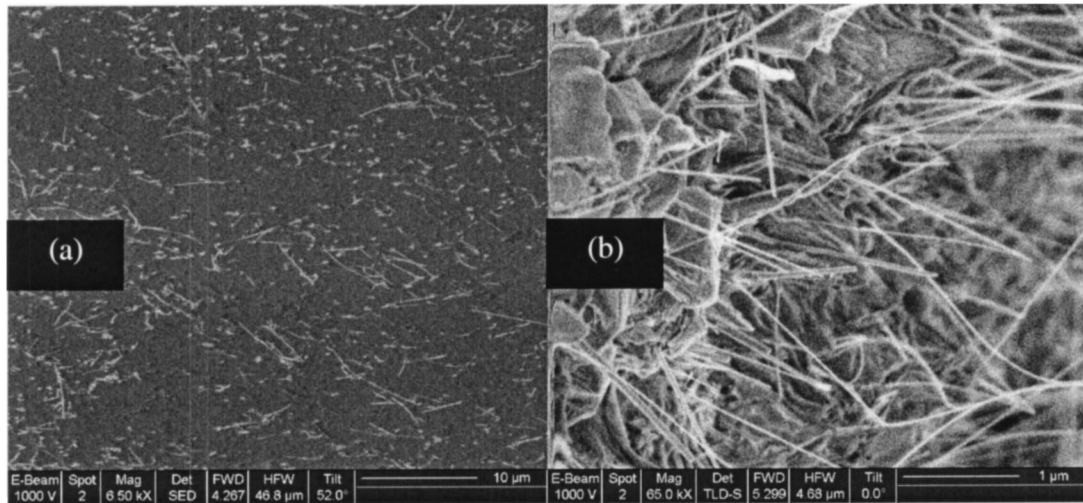


FIG. 1. SEM images of the MWNT-composite film: (a) top view showing the MWNTs are embedded in the polymer matrix while some tubes are still visible on the film surface. (b) The sample was intentionally cracked in half to show that the tubes are uniaxially oriented along the substrate.

This partial orientation of the nanotubes is due to the effect of “hot pressing” during the preparation process. It can also be seen from Fig. 1(b) that there is a variation in the nanotube diameter and length but generally, these tubes are about 10–30 nm in diameter and 3–5 μm long.

Electron field emission measurements were performed using a scanning probe technique. The anode is a 5 mm diameter stainless steel ball bearing suspended directly above the sample. The base pressure of the vacuum chamber was kept below  $5 \times 10^{-6}$  Torr during the measurements. The anode is attached to a stepper motor where the distance between the anode and sample can be varied at a 2.5 μm step size. The anode also has an  $X$ – $Y$  movement of  $25 \times 25$  mm scan area. The anode to sample separation is maintained between 80 and 120 μm during the measurements and the applied voltage was swept from 0 to 2200 V. The gap between the sample and anode is determined by lowering the probe onto the sample surface while a small voltage is applied. Current flow is detected when the probe is in contact with the surface. The macroscopic electric field is defined here as the applied voltage over the anode to sample separation. Threshold electric field ( $E_{th}$ ) is defined as the applied electric field where a FE current of 1 nA is observed. Each sample is measured four times and the threshold field represents the average value of all four measurements. We find that the error bar is within 5%–10%. Mechanical stress was applied to the sample using a simple three-point bending technique shown in Fig. 2. The samples are bent using an optical fibre placed in the middle of the sample and two glass slides then used to clip both ends of the sample to create strain across the sample. Optical fibre diameters ranging from 50 to 1000 μm were used to allow different levels of stresses to be applied to the sample. In this setup, maximum stress is concentrated around the center of the sample above the fiber region and the scanning probe was suspended above this region for FE measurements.

### III. RESULTS AND DISCUSSION

The FE characteristics for MWNT–PS films subject to different mechanical stress are shown in Fig. 3. The control sample, which did not experience any mechanical bending shows an emission threshold field of 2.3 V/μm. The emission current shows an exponential characteristic with applied field, which resembles a Fowler–Nordheim (FN) like emission process. As the mechanical stress increases with the introduction of larger diameter glass fibers ranging from 125 to 500 μm,  $E_{th}$  decreases from 2.3 to 0.6 V/μm. Interestingly, when the glass fiber size is further increased to 1000 μm,  $E_{th}$  for this sample increases from 0.6 to 3.1 V/μm. Current saturation effects are also observed in the emission currents which suggests a ballasting effect of the matrix. Plastic deformation of the sample can be observed after bending the sample at 1000 μm. It was noted that the surface of the sample (not shown here) when subject to the highest deformation results in the melting of the polystyrene if suitable precautions are not taken like using a current limiter. In general, polystyrene turns into plastic from about a temperature of 100 °C and melts at 340 °C. This suggests that when the films are bent at high curvature, me-

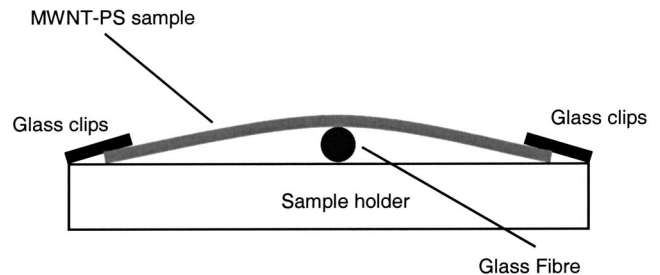


FIG. 2. Experimental setup of the three-point bending stage, where the sample is clamped on both sides with glass clips and the glass fiber size is varied to introduce different curvature.

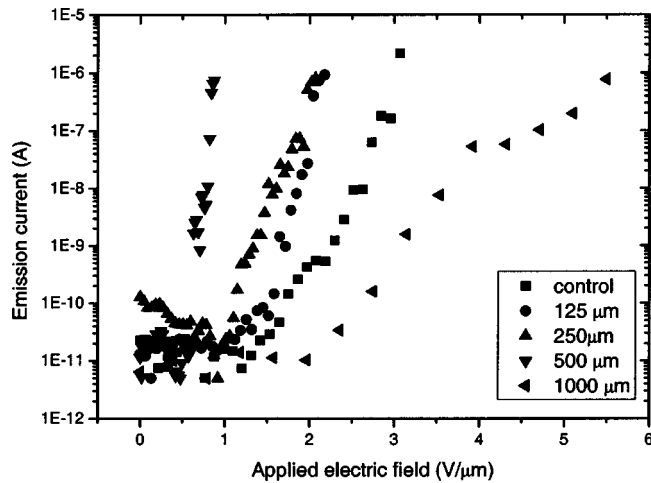


FIG. 3. Field emission current against applied electric field for samples bent with different fiber sizes. Control refers to the field emission characteristic of the sample without mechanical bending.

chanical stress induces changes to the MWNT-PS film resulting in an increase in the sample temperature when subjected to field emission. This is likely to be due to increased localised current conduction around the stressed regions.

The variation in  $E_{th}$  as a function of the fiber size is summarized in Fig. 4. The emission threshold fields in this work are much lower than those reported in the literature. Usually, field emission from materials such as amorphous carbon, emits in the range of 20–30 V/ $\mu\text{m}$ . This again supports the fact that CNTs are excellent electron field emitters. The field emission mechanism is usually explained by FN type emission, and, the high field enhancement is due to the high aspect ratio from these nanosized tubes. This field enhancement factor is related to the height over the tube radius ratio. However, when CNTs are closely packed together, electric field screening effects often affect the emission current and decreases the field enhancement factor. This field screening effect can be minimized by increasing the separation distance between individual tubes. Current saturation effects are also common in field emission from CNTs. This is attributed to the adsorbates on the CNT surface and can be removed by conditioning of the tubes.

Recent work has shown that when CNTs are mixed into polymer, the field emission threshold fields<sup>8</sup> can improve due to the introduction of a triple junction effect. The mixture of the CNT, dielectric, and vacuum creates a space charge region which allows enhanced electron field emission. In this work, we observe that those nanotubes found on the sample surface are mainly short tubes embedded in the polymer (and thus no high enhancement due to  $h/r$ ). The field emission recorded in our films is enhanced by the triple junction effect, which give rise to lower threshold fields.

One possible source as to the improvement in field emission characteristics is the variation in the physical properties when straining the CNTs are subjected to stress. At high stress, it is possible to create “buckling” in the compressively stressed regions.<sup>9</sup> Transmission electron microscopy (TEM)

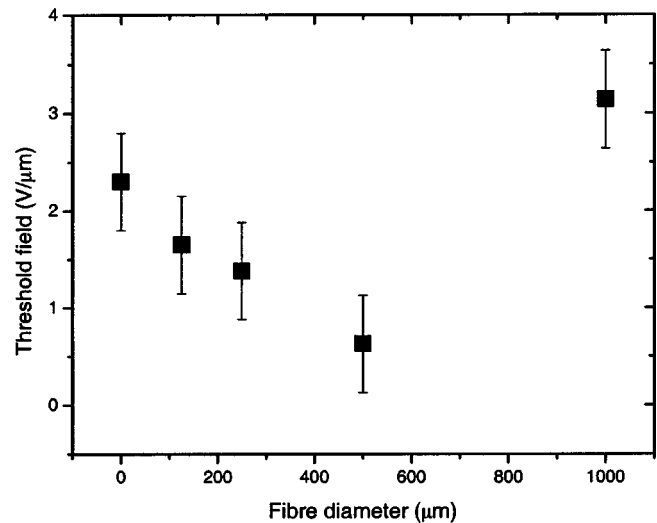


FIG. 4. Variation of threshold fields as a function of different fiber size. The threshold field is defined as the applied field when an emission current of 1 nA is observed.

studies have shown that in strained MWNT-composite films, fractures, and buckling (about 18% and 5%, respectively) are observed. This may suggest that the MWNTs subject to higher curvature is beneficial to the field emission process. Reports have also suggested that CNTs under strain can have an effect on the hybridization. Manipulation of a single walled nanotube shows that deformation along the body of the tube can cause a reversible transition from an  $sp^2$  to an  $sp^3$  bonding configuration in the region subject to the deformation. This leads to a 2 orders of magnitude decrease in the overall conductance.<sup>10</sup> Interestingly, this could mean that the work function along the body of the nanotube could be different when subjected to different degree of stress.

The work function ( $\Phi$ ) of a material is the energy required to extract an electron from the surface. The  $\Phi$  is related to the threshold field in cold-cathode field emission of materials and can be chemically modulated/enhanced by doping with selected impurities.<sup>11</sup> It has been realized that co-doping of O or N with low  $\Phi$  metals can form metal dipoles on the surface and this was suggested to be a promising route<sup>12,13</sup> in lowering the  $\Phi$  at the material surface.

Here we extend our discussion in lowering the work function of CNTs by introducing a lattice contraction argument when the material is mechanically stressed. We extend the current bond-order-length-strength (BOLS) correlation mechanism<sup>14</sup> to the core-level shift in a nanosized material by including the effect surface relaxation and bond contraction. The current BOLS correlation argument indicates that the bond contraction not only deepens the atomic “potential well,” but also enhances the charge density in the relaxed surface region. The confined electrons near the surface edge are usually denser and more localized. For an isolated nanosolid of size  $K_j$ , the  $\Phi$  satisfies  $(V \propto (\bar{d})^\tau)$ ,<sup>15,16</sup> where  $V$  is the volume of a nanosolid,  $\bar{d}$  is related to the bond distance due to lattice contraction, and  $\tau=1, 2,$  or  $3$  is the dimensionality for a plate, rod, and spherical rod, respectively.

The work function is given by  $\Phi = E_0 - E_F$  and the Fermi energy can be derived using

$$E_F \propto n^{2/3} = (N_e/V)^{2/3} \propto (\bar{d})^{-2\pi/3},$$

where  $n$  is the number of electrons. Therefore, the variation in work function can be simplified to

$$\Delta\Phi(K_j) = -\Delta E_F(K_j). \quad (1)$$

If we consider the total number of electrons  $N_e$  of a nanosolid is conserved. At the lower end of the size limit of a spherical or semispherical dot ( $R \sim 1$  nm,  $\tau=3$ ), the average bond length is around 20% shorter than the bulk value and hence the  $\Phi$  will reduce from the original value by 30%, according to Eq. (1). Using an He-II ultraviolet beam source of 21.2 eV, Abbot *et al.*<sup>17</sup> measured the  $\Phi$  of the diamond {111} surface to be about 4.8 eV at a grain size of 108  $\mu\text{m}$ . The  $\Phi$  of the diamond decreases with particle size to a minimum of 3.2 eV at an average grain size of about 4  $\mu\text{m}$ , and then the  $\Phi$  recovers to a maximum of 5.1 eV at diamond particle size of 0.32  $\mu\text{m}$ . Rouse *et al.*<sup>18</sup> noted that the field-emission threshold decreases from 3.8 to 3.4 V/ $\mu\text{m}$  of polycrystalline diamond films at room temperature on molybdenum tips as the diamond average grain size increases from 0.25 to 6  $\mu\text{m}$ . They related the  $\Phi$  change to the increase in negative electron affinity within the grain size due to increased surface hydrogen bonding and with perhaps a contribution from surface defect states. The  $\Phi$  of Na particles around 0.4–2.0 nm in size was measured to vary inversely with the size  $R$  and lowered the bulk value from 2.75 to 2.25 eV (by 18%).<sup>19</sup> The majority of the nanotubes have a  $\Phi$  of 4.6–4.8 eV<sup>20</sup> at the tips, which is 0.2–0.4 eV lower than that of carbon (graphite) bulk. A small fraction of the nanotubes have a  $\Phi$  of  $\sim 5.6$  eV,<sup>20</sup> about 0.6 eV higher than that of carbon (graphite). This discrepancy is thought to arise from the metallic and semiconducting characteristics of the nanotubes.

It appears that the measured size-dependent  $\Phi$  change for diamond is in conflict with the BOLS prediction. However, one needs to note that if the emitters are packed too closely, the system is identical to a smooth surface. It has been found<sup>21</sup> that hydrogen-rich or oxygen-containing chemical vapor deposition (CVD) precursors could promote electron emission from discrete diamond particles and noncontinuous diamond films, but not for high quality and continuous diamond films, nanocrystalline diamond, and glassy carbon coatings even if they contain conductive graphitic carbon. The  $\Phi$  at the tips of individual multiwalled carbon nanotubes was measured using a TEM to show no significant dependence on the diameter of the nanotubes in the range of 14–55 nm.<sup>22</sup> Although the calibrated diamond particles are much larger, the curvature of the tips should be much higher. The particle size corresponds only to the separation of the sharp emitters. This phenomenon indicates the significance

of CN imperfection on the  $\Phi$  reduction that is subject to the separation between the nanoparticles and surface chemical states.

Mechanical stress could raise the atomic binding and the total energy between a pair of atoms, the same effect as of heating and thus weakening the bond. Therefore, heating or straining a nanotube should raise the  $N_e$  higher, and as a consequence, minimize the gap between the  $\pi$  and  $\pi^*$  bands, as proposed by Poa *et al.*<sup>23</sup>

#### IV. SUMMARY

In summary, we have investigated the effects of CNT composite films under stress. Results show that the emission threshold fields of these films can be varied by bending the sample. Threshold fields as low as 0.6 V/ $\mu\text{m}$  have been observed in this work, one of the lowest threshold fields ever reported. This work also suggests the possibility of using CNT-composite films as an electromechanical switch in high power applications.

#### ACKNOWLEDGMENTS

The authors wish to thank Dr. K. Hsu and Professor H. W. Kroto for the supply of the MWNT. They also wish to thank EPSRC for support in the form of a Portfolio Partnership and Carbon Based Electronics programme.

- <sup>1</sup>G. Overney, W. Zhong, and D. Tomanek, *Z. Phys. D: At., Mol. Clusters* **27**, 93 (1993).
- <sup>2</sup>C. T. White and T. N. Todorov, *Nature (London)* **393**, 240 (1988).
- <sup>3</sup>M. Buongiorno Nardelli, B. I. Yakobson, and J. Bernholc, *Phys. Rev. B* **57**, R4277 (1998).
- <sup>4</sup>D. Orlikowski, M. Buongiorno Nardelli, J. Bernholc, and C. Roland, *Phys. Rev. Lett.* **83**, 4132 (1999).
- <sup>5</sup>T. W. Tomblor, C. Zhong, J. Kong, and H. Dai, *Appl. Phys. Lett.* **76**, 2412 (2000).
- <sup>6</sup>R. Heyd, A. Charlier, and E. McRae, *Phys. Rev. B* **55**, 6820 (1997).
- <sup>7</sup>C. H. Poa, S. R. P. Silva, P. C. P. Watts, W. K. Hsu, H. W. Kroto, and D. R. M. Walton, *Appl. Phys. Lett.* **80**, 3189 (2002).
- <sup>8</sup>I. Alexandrou, E. Kymakis, and G. A. J. Amaratunga, *Appl. Phys. Lett.* **80**, 1435 (2002).
- <sup>9</sup>C. Bower, R. Rosen, L. Jin, J. Han, and O. Zhou, *Appl. Phys. Lett.* **74**, 3317 (1999).
- <sup>10</sup>L. Liu, C. S. Jayanthi, M. Tang, S. Y. Wu, T. W. Tomblor, C. Zhou, L. Alexseyev, J. Kong, and H. Dai, *Phys. Rev. Lett.* **84**, 4950 (2000).
- <sup>11</sup>G. A. J. Amaratunga and S. R. P. Silva, *Appl. Phys. Lett.* **68**, 2529 (1996).
- <sup>12</sup>W. E. Pickett, *Phys. Rev. Lett.* **73**, 1664 (1994).
- <sup>13</sup>L. W. Lin, *J. Vac. Sci. Technol. A* **6**, 1053 (1998).
- <sup>14</sup>C. Q. Sun, B. K. Tay, X. T. Zeng, S. Li, T. P. Chen, J. Zhou, H. L. Bai, and E. Y. Jiang, *J. Phys.: Condens. Matter* **14**, 7781 (2002).
- <sup>15</sup>C. Q. Sun *et al.*, *J. Appl. Phys.* **90**, 2615 (2001).
- <sup>16</sup>C. Q. Sun, *Phys. Rev. B* **69**, 045105 (2004).
- <sup>17</sup>P. Abbott, E. D. Sosa, and D. E. Golden, *Appl. Phys. Lett.* **79**, 2835 (2001).
- <sup>18</sup>A. A. Rouse, J. B. Bernhard, E. D. Sosa, and D. E. Golden, *Appl. Phys. Lett.* **75**, 3417 (1999).
- <sup>19</sup>M. M. Kappes and E. Schuhmacher, *Ber. Bunsenges. Phys. Chem.* **88**, 220 (1984).
- <sup>20</sup>R. Gao, Z. Pan, and Z. L. Wang, *Appl. Phys. Lett.* **78**, 1757 (2001).
- <sup>21</sup>Y. Tzeng, C. Liu, and A. Hirata, *Diamond Relat. Mater.* **12**, 456 (2003).
- <sup>22</sup>R. Gao, Z. Pan, and Z. L. Wang, *Appl. Phys. Lett.* **78**, 1757 (2001).
- <sup>23</sup>C. H. Poa, R. G. Lacerda, D. C. Cox, S. R. P. Silva, and F. C. Marques, *Appl. Phys. Lett.* **81**, 853 (2002).